Hopf Bifurcation to Convection near the Codimension-Two Point in a ^{3}He-^{4}He Mixture

Timothy S. Sullivan and Guenter Ahlers

Department of Physics, University of California, Santa Barbara, Santa Barbara, California 93106

(Received 24 February 1988)

From measurements of the convective heat transport in a normal ^{3}He-^{4}He mixture over the range $-0.018 \lesssim \psi \lesssim 0.015$ of the separation ratio ψ, we found a time-periodic state for $\psi < \psi_{CT} = -0.0044$. The dimensionless onset frequency at ψ_{CT} was 1.42, much larger than the value predicted by linear-stability analysis for a spatially uniform, laterally infinite system. For $\psi_{CT} > \psi > \psi_c \approx -0.010$ the bifurcation to oscillations was forward while for $\psi \lesssim \psi_c$ it was backward. The results suggests that ψ_c is an additional codimension-two point, rather than a Hopf tricritical point.

PACS numbers: 47.20.−k, 47.25.Qv

The stability to infinitesimal perturbations of a pure conduction state in a fluid mixture heated from below is a linear problem which in principle can be solved with arbitrary accuracy. Nonetheless we find that experimental measurements near the onset of convection in a binary mixture disagree dramatically with the predictions of linear-stability analysis.[1] We presume that this difficulty arises from one of the assumptions which enters into the theoretical calculation. The most likely candidate, it seems to us, is the assumption that the convecting state will be spatially uniform. However, it is not at all clear whether and how this spatial variation should influence the *linear* stability.

Convection in binary mixtures heated from below has become a prototype for the study of a great variety of linear and nonlinear phenomena because a richness of behavior can be produced by the variation of *two* external control parameters. One of these is the Rayleigh number R which is proportional to the temperature difference ΔT across the sample. The other is the separation ratio ψ which determines whether mass diffusion helps ($\psi > 0$) or hinders ($\psi < 0$) convection. Of particular interest has been the occurrence in this system of a codimension-two point at (R_{CT}, ψ_{CT}) where a line of Hopf bifurcations from conduction to time-periodic traveling-wave[2] (TW) convection for $\psi < \psi_{CT}$ meets a line of stationary bifurcations from conduction to time-independent convection for $\psi > \psi_{CT}$ (see Fig. 2 below).[2,3] Away from ψ_{CT} interesting spatial variations of the TW envelope have been observed.[4] Close to ψ_{CT} the competition between the TW state and the stationary convection state presents further possibilities for interesting behavior which have yet to be explored in detail. Every theoretical work[5] had yielded the prediction that the frequency ω_0 of the time-periodic state which forms along the Hopf bifurcation line should vanish at ψ_{CT}. More recent linear-stability analyses for a spatially uniform, laterally infinite system have yielded a nonzero $\omega_0(\psi_{CT})$,[1] but for the parameters relevant to mixtures which have been used in experiments $\omega_0(\psi_{CT})$ is predicted to be very small (of order 10^{-1} when time is scaled by the vertical thermal diffusion time). We find that $\omega_0(\psi_{CT}) \approx 1.4$, i.e., over an order of magnitude larger than the predicted value. Thus there is an apparent disagreement between experiment and linear theory. Although we have been unable to establish with certainty the reason for the discrepancy, we think that it will be found in an intrinsic spatial nonuniformity of the traveling-wave convecting state[4] or an instability of the TW envelope.

The oscillatory state for $\psi < \psi_{CT}$ has also attracted considerable attention. Close to ψ_{CT} we find that the Hopf bifurcation to this state is not hysteretic, and thus we presume that it is forward. However, for $\psi < \psi_c \approx -0.010$, the Hopf bifurcation is hysteretic and thus backward. A transition from a forward to a backward bifurcation as ψ is decreased through ψ_c has been predicted for this system.[6] However, this transition is expected to occur smoothly via a tricritical bifurcation, whereas we find the change to be precipitous, suggesting that ψ_c is yet another codimension-two point. We presume that ψ_c is associated with a change in the wave

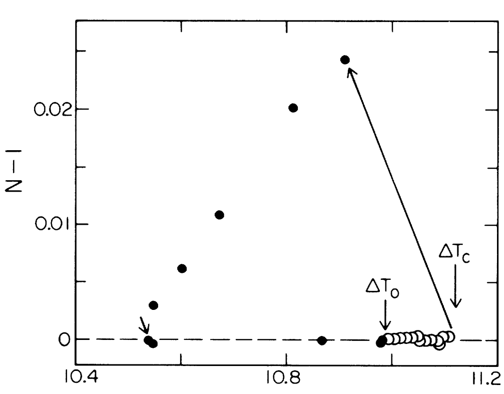

FIG. 1. Convective heat transport $N-1$ as a function of temperature difference ΔT across the cell, for $\psi = -0.0092$. Filled circles indicate time-independent N, open circles indicate time-dependent N, and arrows indicate a hysteretic bifurcation.

number of the TW state, but believe that an explanation is required as to why this should occur in conjunction with the transition from a forward to a backward bifurcation.

The apparatus and convection cell were similar to ones used previously.[7,8] The cell had a height $d=0.083$ cm, length $34d$, and width $6.9d$. We express our results in terms of $N-1$, where the Nusselt number N is the measured thermal conductance normalized by the conductance of the nonconvecting state. All times and frequencies were normalized by the vertical thermal diffusion time $t_v = d^2/\kappa$. The fluid and the relation $\psi(T)$ were the same as those of two previous experiments.[7,8]

Figure 1 displays the dependence of $N-1$ on the temperature difference ΔT across the cell for $\psi = -0.0092$. Starting from a conductive state at small ΔT the first bifurcation (at ΔT_0) was to a state with time-dependent thermal conductance denoted in Fig. 1 by the open circles. On the scale of Fig. 1, the enhanced heat transport of this state is too small to be noticeable. At ΔT_c, this state became unstable at a backward bifurcation (long arrow) to a large-amplitude ($N-1 \approx 10^{-2}$) state whose thermal conductance was time independent. To return to the state of pure conduction, ΔT had to be reduced to the point indicated by the short arrow.

The location in the ΔT-ψ plane of the observed bifurcation sequence is shown in Fig. 2. For $\psi < -0.0044$ the solid line indicates the onset $\Delta T_0(\psi)$ of time-dependent convection, and the dash-dotted line shows where the time-dependent state made a transition to the time-independent (stationary) convection state (ΔT_c in Fig. 1). For $-0.0044 < \psi < 0.0035$ no time-dependent state was observed; rather, the conduction state became unstable at a backward bifurcation directly to stationary convection at the long-dashed line. In order to return from stationary convection to conduction, ΔT had to be reduced to the short-dashed line. For $\psi > 0.0035$, the bifurcation to stationary convection was forward.[9] We identify the intersection of the solid line and the dashed line at $\psi = \psi_{CT} = -0.0044$ as the codimension-two point.

The nature of the time-dependent state for the range of ψ in Fig. 2 is shown by an example in Fig. 3. In Fig. 3(a) a portion of a time series (whose total length was $800t_v$) is shown for $\psi = -0.0092$, $\epsilon = (4.1 \pm 0.4) \times 10^{-3}$, where $\epsilon \equiv (\Delta T - \Delta T_0)/\Delta T_0$. Most of the time dependence is instrumental noise. However, a Fourier transform [Fig. 3(b)] reveals two significant peaks, at $\omega_1 = 1.76$ and $\omega_2 = 2\omega_1$.[10] For comparison, the horizontal bar in Fig. 3(a) has a length corresponding to one period for ω_1. The amplitude of the oscillations in N is only about 10^{-5}. The day-to-day variations in the thermometry gave an uncertainty of order 10^{-4} in the mean Nusselt number. This necessitated the use of transient measurements, stepping ΔT from conduction to a point in the time-dependent regime, to show that the mean conductance in this state had a magnitude $N-1 \approx 2 \times 10^{-4}$. Thus the oscillations modulated the convected heat transport by roughly 5% of the mean value. This behavior is consistent with that expected of a traveling-wave state of finite spatial extent. The instrumental noise prevented measurement of any time evolution of the frequency during the transient.

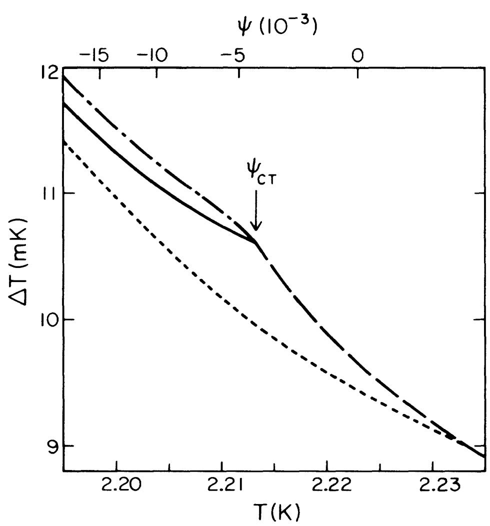

FIG. 2. Bifurcation diagram showing the locations of transitions between conduction and time-dependent convection (solid line), time-dependent convection and stationary convection (dash-dotted line), conduction to stationary convection (long-dashed line), and the return to conduction from stationary convection as the temperature difference is reduced (dashed line).

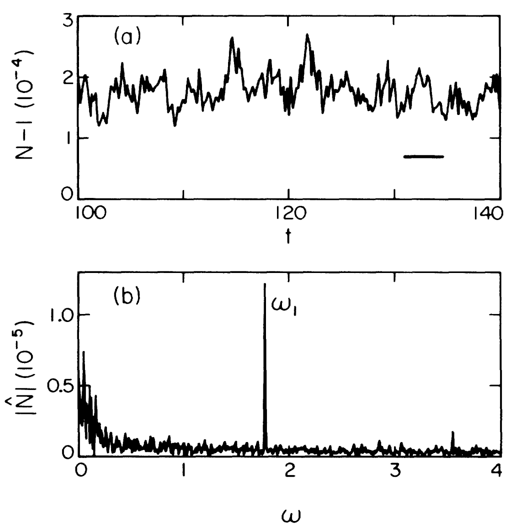

FIG. 3. (a) A portion of a time series for the convective heat transport $N-1$ (of total length 800) for $\psi = -0.0092$ and $\epsilon = (4.1 \pm 0.4) \times 10^{-3}$. The data are dominated by instrumental noise. The horizontal bar has a length corresponding to one period for $\omega = 1.76$. (b) Absolute value of the Fourier transform $\hat{N}$ of the complete time series for $N-1$ of which (a) is a part.

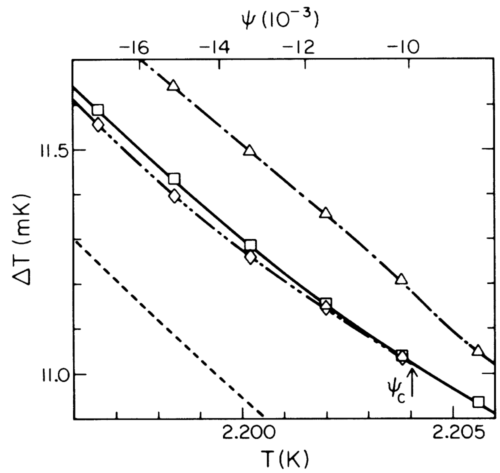

FIG. 4. An enlargement of the bifurcation diagram (Fig. 2) showing the region where the transition to time-dependent convection changed from forward to backward. Squares, onset of time dependence as ΔT was increased; lozenges, disappearance of time dependence as ΔT was decreased; triangles, time-dependent state lost stability to stationary convection as ΔT was increased; short-dashed line, stationary convection lost stability to conduction as ΔT was decreased.

Figure 4 is an enlargement of the bifurcation diagram showing the region where the bifurcation to time dependence changes from forward to backward. As ΔT was increased, periodic time dependence was first observed at the square symbols. As ΔT was decreased, the time dependence ceased at the lozenge symbols. The time-dependent state made a hysteretic transition to stationary convection at the triangles. The onset of time dependence was seen to be nonhysteretic for $\psi_c < \psi < \psi_{CT}$ and hysteretic (and thus backward) for $\psi < \psi_c$ with $\psi_c = -0.010$.

Figure 5 shows ω_1 (see Fig. 3) as a function of ΔT for $\psi = -0.0089$. If the bifurcation to the time-dependent state is forward, then an extrapolation of ω_1 to ΔT_0 gives the Hopf bifurcation frequency, which may be compared with the results of linear-stability analysis. This extrapolation is shown in Fig. 6 by the square symbols for $\psi_c < \psi < \psi_{CT}$. For completeness, we have also plotted ω_1 where the time dependence ceased (as ΔT was reduced) as the lozenge symbols for $\psi < \psi_c$. Also displayed, as the triangles, is ω_1 at the bifurcation to stationary convection (ΔT_c in Fig. 5). The triangles at $\omega = 0$ indicate values of ψ where no time dependence was seen. The solid line shown is the Hopf bifurcation frequency for a linear-stability analysis of a laterally infinite, spatially uniform system.[1] In the range $\psi_c < \psi < \psi_{CT}$ where the bifurcation to time dependence is forward (filled squares) Fig. 6 reveals rather good agreement between theory and experiment. However, there are two major differences. In the ideal system, the intersection of the stationary and oscillatory instability lines occurs at $\psi_{CT} = -0.00054$ rather than the experimentally determined value of $\psi_{CT} = -0.0044$. Although we think that there is a genuine discrepancy, one might attribute part of this difference to effects associated with departures from the Boussinesq approximation and with barodiffusion,[11] and to inaccuracies in the relation $\psi(T)$

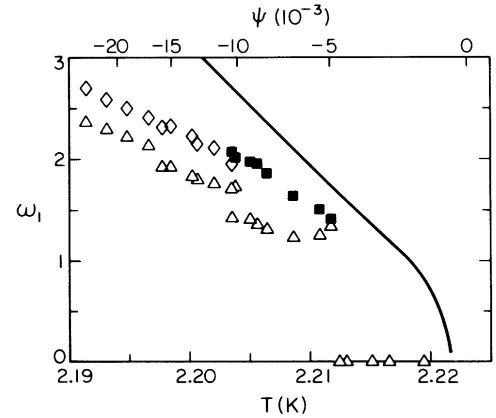

FIG. 6. Comparison of the experimentally determined Hopf bifurcation frequency ω_0 (squares) with that calculated in Ref. 1 (solid line). Also shown is the frequency at the instability to stationary convection (triangles) and the frequency where time dependence ceased as ΔT was reduced when the bifurcation to the oscillatory state was backwards (lozenges).

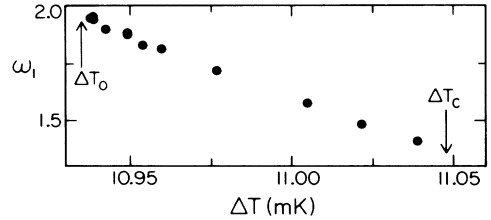

FIG. 5. Variation of the peak frequency ω_1 in the Fourier transform with ΔT for $\psi = -0.0089$.

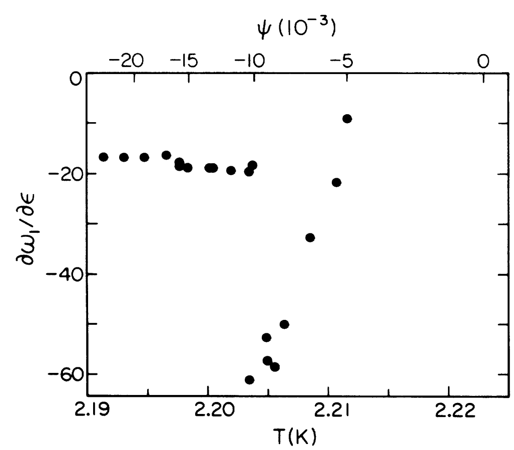

FIG. 7. Slope of $\omega_1(\Delta T)$ (see Fig. 5) as a function of ψ.

used in the experiment. The second difference is not as easily explained. The linear-stability analysis yields $\omega_0 \approx 0.1$ at ψ_{CT}, whereas the experimental value is 1.42. This cannot be attributed to non-Boussinesq effects, barodiffusion, or forcing in the experiment. These effects were as large or larger in previous measurements on the same mixture in a porous medium,[7] which yielded a very small or vanishing frequency at ψ_{CT}.

Another difference between experiment and theory[6] exists along the Hopf bifurcation line near ψ_c. According to the predictions, the Hopf bifurcation changes from forward to backward via a tricritical bifurcation. This phenomenon can be described[12] for a spatially uniform system by the Landau amplitude equation $\tau_0 \dot{A} = \epsilon A - g|A|^2 A - k|A|^4 A$, with τ_0 and ϵ real but $g(\psi)$ and $k(\psi)$ complex. In that case one may show that $(\partial\omega_1/\partial\epsilon)_{\epsilon=0}$ diverges as $-|\psi-\psi_c|^{-1}$ on either side of ψ_c. We show in Fig. 7 the slope $\partial\omega_1/\partial\epsilon \equiv \Delta T_0[\partial\omega_1/\partial(\Delta T)]$ of data like those in Fig. 5, at various values of ψ. For $\psi > \psi_c$, this slope decreases rapidly as ψ_c is approached; but for $\psi < \psi_c$ the slope is essentially constant. Thus, the experimentally observed behavior of $\partial\omega_1/\partial\epsilon$ is quite different from that expected for a tricritical Hopf bifurcation. We conjecture instead that the transition at ψ_c is another codimension-two point associated with a change in the wave vector of the traveling waves, which was not considered in the Landau description discussed above and had not been detected in the theoretical analysis.[6]

We wish to thank E. Knobloch and D. R. Moore for supplying us with their calculations of $\omega_0(\psi)$ well in advance of publication. This work was supported by the National Science Foundation through Grant No. DMR-84-14804.

[1]S. J. Linz and M. Lücke, Phys. Rev. A **35**, 3997 (1987), and **36**, 2486(E) (1987); E. Knobloch and D. R. Moore, to be published; M. C. Cross and K. Kim, to be published; B. J. A. Zielinska and H. R. Brand, Phys. Rev. A **35**, 4349 (1987), and **37**, 1786(E) (1988).

[2]E. Knobloch, Phys. Rev. A **34**, 1538 (1986), and references therein.

[3]D. T. J. Hurle and F. Jakeman, J. Fluid Mech. **47**, 667 (1981); D. Gutkowicz-Krusin, M. A. Collins, and J. Ross, Phys. Fluids **22**, 1443, 1451 (1979).

[4]R. Heinrichs, G. Ahlers, and D. S. Cannell, Phys. Rev. A **35**, 2761 (1987); G. Ahlers, D. Cannell, and R. Heinrichs, Nucl. Phys. (Proc. Suppl.) **B2**, 77 (1987); E. Moses, J. Fineberg, and V. Steinberg, Phys. Rev. A **35**, 2757 (1987).

[5]H. R. Brand, P. C. Hohenberg, and V. Steinberg, Phys. Rev. A **30**, 2548 (1984).

[6]S. J. Linz and M. Lücke, in Propagation in Non-Equilibrium Systems, edited by J. E. Wesfreid, H. R. Brand, P. Manneville, G. Albinet, and N. Boccara, Springer Series in Physics (Springer-Verlag, Berlin, to be published).

[7]I. Rehberg and G. Ahlers, Phys. Rev. Lett. **55**, 500 (1985), and Contemp. Math. **56**, 277 (1986).

[8]G. Ahlers and I. Rehberg, Phys. Rev. Lett. **56**, 1373 (1986).

[9]This result confirms the conclusion of Ref. 8 that the tricritical point is located at $\psi > 0$. The different sample thickness and ΔT_c rule out an explanation based on non-Boussinesq effects.

[10]In Ref. 8, ΔT_c was smaller and Fourier transform techniques were not employed. Therefore the oscillations, which had an amplitude of less than 1 μK, were not detected. With the use of Fourier transforms, our resolution for oscillation amplitudes is now 10^{-8} K.

[11]S. J. Linz and M. Lücke, Phys. Rev. A **36**, 3505 (1987).

[12]H. Brand and V. Steinberg, Phys. Lett. **93A**, 333 (1983), and references therein.